RSC Advances

ROYAL SOCIETY OF CHEMISTRY

www.rsc.org/advances

Effect of 4,4'-Stilbenedicarboxylic acid-intercalated layered double hydroxides on UV aging resistance of bitumen

Chao Peng[a,*], Guosheng Jiang[a], Chunhua Lu[a], Fang Xu[a], Jianying Yu[b], Jing Dai[c]

([a]*Faculty of Engineering, China University of Geosciences, Wuhan, 430074, PR China*

[b]*State Key Laboratory of Silicate Materials for Architectures, Wuhan University of Technology, Wuhan 430070, PR China*

[c]*Key Laboratory of Advanced Technology for Special Functional Materials of Ministry of Education, Wuhan 430070, PR China*)

Abstract: UV aging is the main cause of the deterioration of bitumen pavement. To mitigate the aging process, a nanohybrid prepared by intercalation of 4,4'-Stilbenedicarboxylic acid (SA) into Zn/Al layered double hydroxide (LDH) was blended with styrene-butadiene-styrene (SBS) bitumen. The results of X-ray diffraction, Fourier transform infrared spectroscopy (FTIR) and transmission electron microscopy showed that SA anions have been successfully intercalated into the LDH galleries and the interlayer distance of LDH increased from 0.76nm to 1.37nm. UV-vis spectroscopy measurement revealed that the Zn/Al LDH intercalated with SA anions (Zn/Al-SA-LDH) has a synergistic effect on reflecting and adsorbing UV light. The physical tests, FTIR analysis and atomic force microscopy images of the bitumen specimens proved that the UV aging resistance of SBS modified bitumen can be significantly enhanced by Zn/Al-SA-LDH.

1. Introduction

Bitumen, which is an important byproduct of crude oil, has been widely used as a binder of mineral aggregates in road pavements due to its viscoelastic properties.[1] However, bitumen is an organic material, which is easily degraded by ultraviolet (UV) radiation, oxygen and heat. This typical aging process results in a more brittle bitumen, which is subject to low-temperature cracking, and eventually the lifespan of pavement is shorten.[2,3]

*Corresponding author at E-mail: pengchao@cug.edu.cn

To mitigate this degradation effect, a number of methods have been developed by many researchers. Lu et al found that the addition of Styrene-Butadiene-Styrene (SBS) improved the rheological properties of bitumen after thermal-aging.[4] De Filippis et al reported that the distillation bitumen mixed with small quantities of phosphoric acid had a better aging resistance than pristine bitumen.[5] Ouyang et al investigated the effects of antioxidants on aging resistances for base and SBS modified bitumens. The results showed that antioxidants could retard the aging process of bitumens.[6] Dessouky et al revealed that the stripping resistance and rutting performance of polymer-modified bitumen were enhanced by adding hindered phenol.[7] Cong et al noticed that carbon black was helpful in improving short-term and long-term aging resistances of SBS modified bitumen.[8] Yu et al disclosed that of sodium montmorillonite and organophilic montmorillonite had beneficial effects on the improvement of thermal aging resistance of SBS modified bitumen.[9]

During the recent years, Layered double hydroxide (LDH) has been used as a bitumen modifier to block UV light due to the multi-layered structure, and thus the UV aging process could be delayed to some extent.[10] However, like other inorganic materials, the compatibility between the inherently hydrophilic LDH and organic bitumen is unsatisfactory. Therefore, it is essential to transform the hydrophilic LDH to the hydrophobic LDH by inserting organic anions into LDH galleries.

The applications of UV absorbers/LDH hybrids in polymer materials have attracted a considerable attention. For examples, these hybrids have a significant effect on blocking UV light in PVC, PP, PVA and so on.[11-13] Accordingly, incorporating UV absorbers into LDH has a good potential to improve the UV aging resistance of bitumen.

In this article, a UV absorber called 4,4'-Stilbenedicarboxylic acid was initially intercalated into zinc/aluminum LDH (Zn/Al LDH) by the re-construction method. Then Zn/Al LDH specimens were used to modify bitumen and UV aging resistances of modified bitumen specimens were investigated by physical tests, Fourier transform infrared (FTIR) spectrometer and atomic force microscopy (AFM).

2. Experimental

2.1 Materials

Analytic grade chemical agents are including $Zn(NO_3)_2 \cdot 6H_2O$, $Al(NO_3)_3 \cdot 9H_2O$, NaOH and 4,4'-Stilbenedicarboxylic acid (SA), which were produced from Shanghai Chemical Industrial Company (Shanghai, China). Styrene-butadiene-styrene (SBS) modified bitumen was provided by China Best Modified Bitumen Co. LTD (Hubei, China), with softening point of 47.5°C (ASTM D36), penetration of 69 dmm (ASTM D5), ductility of 89.6 cm (ASTM D4402) and viscosity of 0.52 Pa.s (ASTM D4402), was provided by China Best Modified Bitumen Co. LTD (Hubei, China). The chemical structure of SA is shown in Fig. 1.

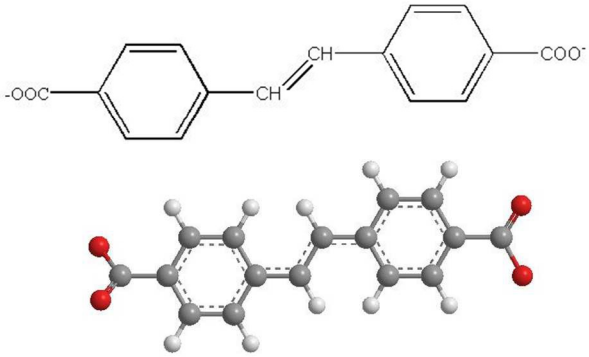

Fig. 1 Chemical structure of SA

2.2 Preparation of Zn/Al–SA-LDH

$Zn_4Al_2(OH)_{12}CO_34H_2O$ (denoted as Zn/Al-CO_3^{2-}-LDH) precursor was prepared by co-precipitation method, as described in the previous literature.[14] Zn/Al–SA-LDH were manufactured by the calcination recovery method. Firstly, 200 g of Zn/Al-CO_3^{2-}-LDH was calcined in a muffle furnace at 500°C for approximately 4h to remove the CO_3^{2-} anions. Secondly, the decarbonated LDH (DLDH) was cooled in a closed storage pan, which was under CO_2-free atmosphere using a vacuum pump. Subsequently, 300 ml of SA solution (concentration of 20 wt%) and DLDH were mixed in a glass flask, followed by agitation at 80 °C for 1h. Finally, the resulting mixture was filtrated and washed with hot distilled water several times. and dried at 105 °C for 24h. The schematic illustration of preparation process is shown in Fig. 2.

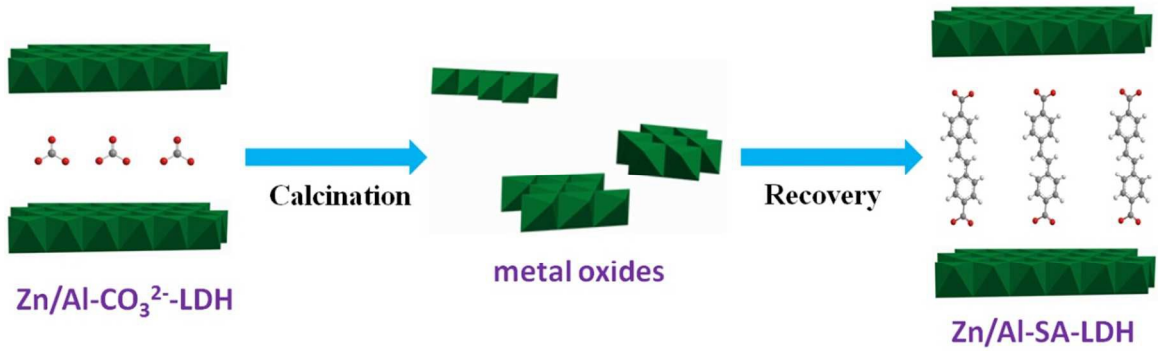

Fig. 2 Preparation of Zn/Al-SA-LDH

2.3 Preparation of bitumen specimens

Bitumen was heated to become a well fluid at 150 °C in a metal container, and then 5 wt% Zn/Al-SA-LDH or Zn/Al-CO_3^{2-}-LDH was added into SBS modified bitumen at a shearing speed of 4000 rpm for about 60 min to ensure a homogenous dispersion. Pristine SBS modified bitumen undergone the similar procedure due to the thermal aging of bitumen during the heating process.[15]

2.4 UV aging process

The UV accelerating aging tests was conducted in a chamber equipped with a UV lamp, which had a UV light wavelength of 365 nm and a UV irradiation intensity of 1200μW/cm^2. Bitumen specimens were poured into stainless steel pans (Φ140±0.5 mm), and the thickness of bitumen films were approximately 3.0 mm. These pans containing bitumen specimens were placed in the UV chamber at 60 °C for 12 days.

2.5 Characterization

A FTIR spectrometer from Thermo Nicolet Corp. (New York, USA) was used to record the spectra of Zn/Al-CO_3^{2-}-LDH, Zn/Al-SA-LDH and their modified bitumen specimens before and after UV aging process. Spectra were recorded in the range of 400 cm^{-1} and 4000 cm^{-1} and the resolution was 4 cm^{-1}. A X-ray diffractometer (XRD) from Rigaku Corp. (Tokyo, Japan), with a CuKα radiation (λ=0.15406 nm; 40 kV, 50 mA), was used to collect the patterns of Zn/Al-CO_3^{2-}-LDH, Zn/Al-SA-LDH. The scan range was from 2 ° to 20 ° and the scanning rate was 2 °/min. To investigate the dispersion condition of Zn/Al-CO_3^{2-}-LDH and Zn/Al-SA-LDH in bitumen, trichloroethylene was used to extract

Zn/Al-CO_3^{2-}-LDH and Zn/Al-SA-LDH form bitumen matrix. The extraction procedure was performed as follows: Zn/Al-CO_3^{2-}-LDH/SBS modified bitumen or Zn/Al-SA-LDH/SBS modified bitumen was washed and filtered by trichloroethylene several times. The residual solids were next placed in an oven at 85 °C until trichloroethylene was completely evaporated and the dried products were ground to obtain the extracted Zn/Al-CO_3^{2-}-LDH and Zn/Al-SA-LDH. A transmission electron microscopy (TEM) from JEOL Corp. (Tokyo, Japan) was used to observe the morphologies of Zn/Al–CO_3^{2-}-LDH and Zn/Al–SA-LDH. The accelerating voltage was 200 kV and all the specimens were coated with platinum before TEM observation. A UV spectrometer from Shimadzu Corp. (Kyoto, Japan) was used to obtain the UV-Vis absorbance and reflection spectra of Zn/Al–CO_3^{2-}-LDH and Zn/Al–SA-LDH. An AFM from Veeco Corp. (New York, USA) was used to observe the microstructures of bitumen specimens before and after UV aging process.

2.6 Physical tests of bitumen

The physical properties of pristine SBS modified bitumen, Zn/Al–CO_3^{2-}-LDH/SBS modified bitumen and Zn/Al–SA-LDH/SBS modified bitumen, including penetration and softening point, were measured following the standards of ASTM D5 and ASTM D36.

3. Result and Discussion

3.1 FTIR analysis

FTIR spectra of SA, Zn/Al–CO_3^{2-}-LDH and Zn/Al–SA-LDH are shown in Fig.3. In the spectrum of Zn/Al–CO_3^{2-}-LDH (shown in Fig. 3a), a broad peak observed at around 3451 cm^{-1} is due to the stretching vibration of -OH groups from interlayer water molecules or brucite-like layers. A strong peak centered at 1384 cm^{-1} is caused by the stretching vibration of CO_3^{2-} and peaks appeared at around 436 cm^{-1} are ascribed to M-O vibrations in metal layers of LDH.[16,17] In the spectrum of SA (shown in Fig. 3b), the broad peak between 2500 and 3000 cm^{-1} is attributed to the stretching vibration of the -COOH and the characteristic peak at 1677 cm^{-1} is associated with the C=O vibration.[18] In the spectrum of Zn/Al–SA-LDH (shown in Fig. 3c), the characteristic peak corresponding to the -COOH vibration disappears, indicating that SA anions have been intercalated into

the interlayer spaces of LDH. Compared with the spectrum of Zn/Al–CO_3^{2-}-LDH, the spectrum of Zn/Al-SA-LDH shows a stronger adsorption peak of -OH group at 3392 cm^{-1} due to the re-construction process in aqueous condition, this also implies that the intensity of -OH groups have been increased. In addition, the absence of CO_3^{2-} absorption peak in the spectrum of Zn/Al–SA-LDH confirms that the CO_3^{2-} anions have been fully replaced by SA anions.

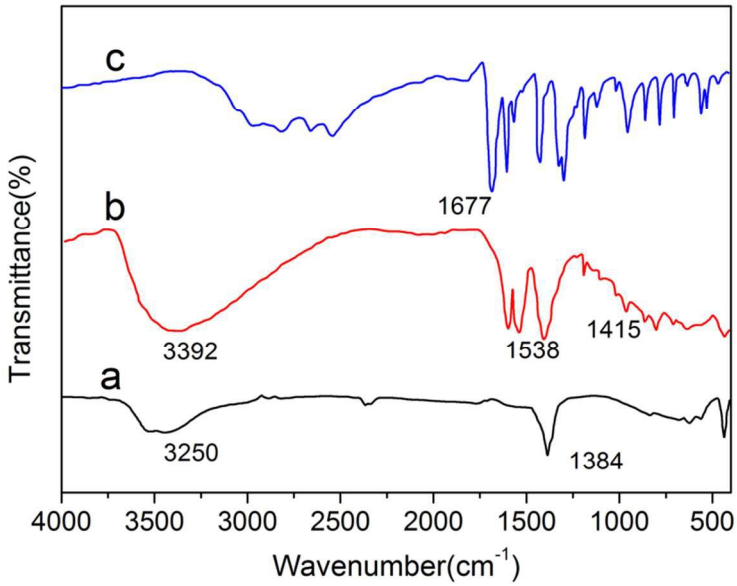

Fig. 3 FTIR patterns of (a) Zn/Al-CO_3^{2-}-LDH, (b) Zn/Al-SA-LDH and (c) SA

3.2 XRD

XRD diffraction patterns of Zn/Al-CO_3^{2-}-LDH and extracted Zn/Al-CO_3^{2-}-LDH are presented in Fig. 4(a). It can be seen that the characteristic peaks appeared at 2θ of 11.67° are ascribed to the first basal reflections (001) of Zn/Al-CO_3^{2-}-LDH and extracted Zn/Al-CO_3^{2-}-LDH, respectively. According to the Bragg equation ($\lambda=2d\cdot Sin\theta$, λ=1.542 Å), the interlayer distance (d) can be calculated. The interlayer distances of Zn/Al-CO_3^{2-}-LDH and extracted Zn/Al-CO_3^{2-}-LDH are both 0.76 nm, indicating that the interlayer distance does not change when Zn/Al-CO_3^{2-}-LDH particles are dispersing in bitumen. In other words, Zn/Al-CO_3^{2-}-LDH/SBS modified bitumen forms a separated phase structure which is shown in Fig. 4(b). Fig. 4(c) presents the XRD diffraction patterns of Zn/Al-SA-LDH and extracted Zn/Al-SA-LDH. The (001) peak of

Zn/Al-SA-LDH pattern appeared at 2θ of 5.73° with a interlayer distance of 1.54 nm, which is much wider than the interlayer distance of Zn/Al-CO_3^{2-}-LDH (0.76 nm). For the extracted Zn/Al-SA-LDH, the (001) peak can be observed at 2θ of 4.47° with a interlayer distance of 1.98 nm, indicating that bitumen molecules have entered into LDH galleries and Zn/Al-SA-LDH/SBS modified bitumen forms a expanded phase structure which is displayed in Fig. 4(d). Comparing these two dispersion structures of Zn/Al-CO_3^{2-}-LDH and Zn/Al-SA-LDH in bitumen matrix, it can be deduced that compatibility between Zn/Al-SA-LDH and bitumen has been improved remarkably.

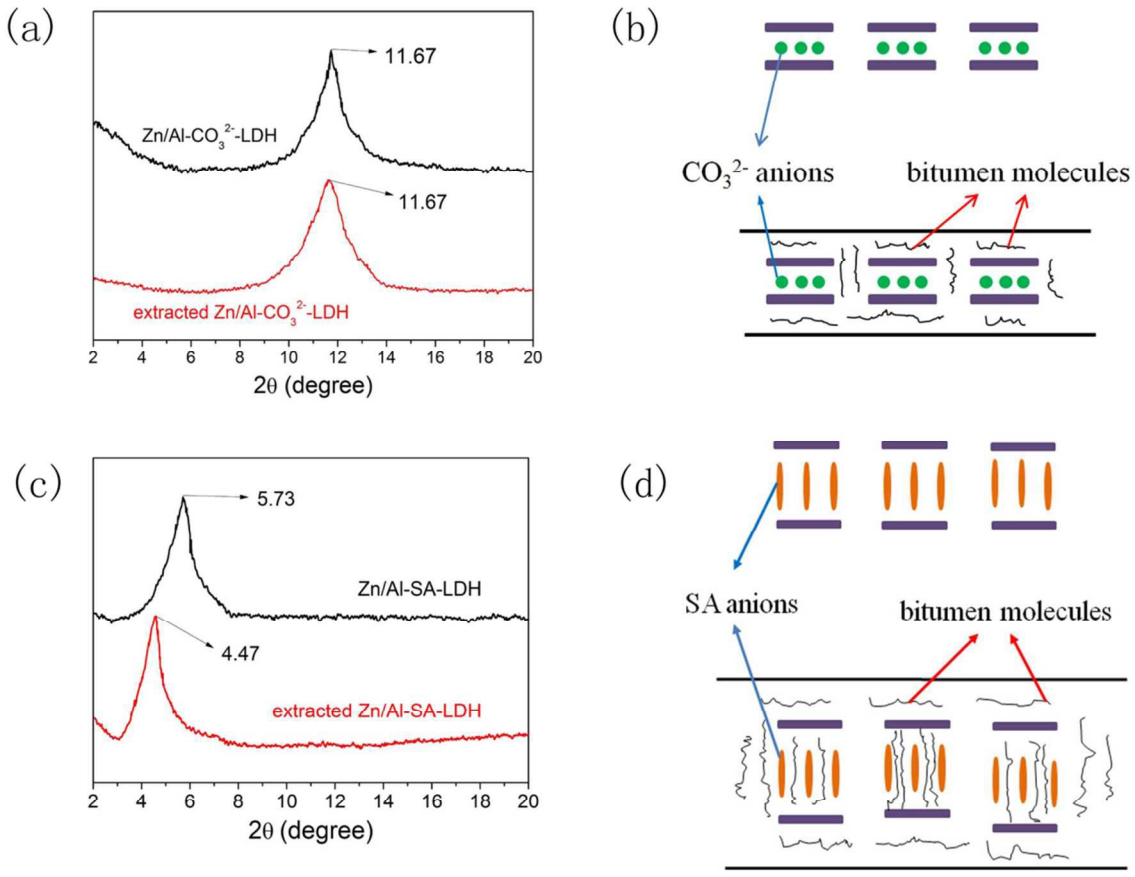

Fig. 4 Typical XRD patterns and schematic models of (a, b) Zn/Al-CO_3^{2-}-LDH and (c, d) Zn/Al-SA-LDH

3.3 TEM observation

The TEM micrographs of Zn/Al-CO_3^{2-}-LDH and Zn/Al-SA-LDH are shown in Fig. 5. From the Fig. 5(a), it can be seen that the Zn/Al-CO_3^{2-}-LDH crystals are composed of

hexagonal sheets with smooth surface and the dimension of crystals is in the range of 400-500 nm. Fig. 5(c) shows that the crystal shape of Zn/Al-SA-LDH is less uniform than that of Zn/Al-CO_3^{2-}-LDH and some defects appeared at the edges of crystallites. This is because Zn/Al-SA-LDH crystallites have restored their laminar structure due to the memory effects of LDH. Figs. 5(b) and (d) display that the interlayer distances of Zn/Al-CO_3^{2-}-LDH and Zn/Al-SA-LDH are 0.76 and 1.54 nm, which are in accordance with the results from the XRD analyses. Meanwhile it further confirms that the introduction of SA increases the interlayer distance of pristine LDH.

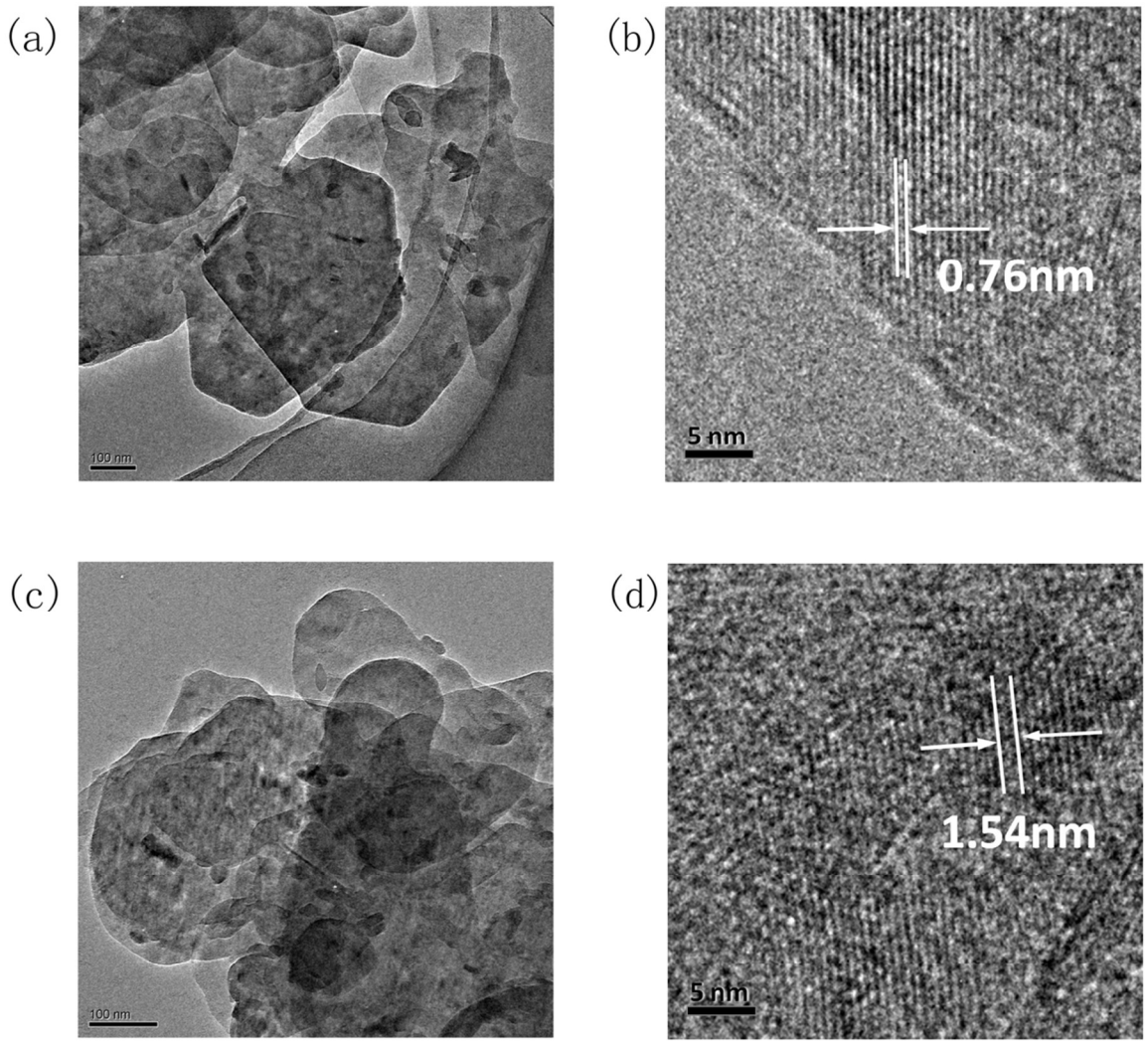

Fig. 5 TEM images of (a, b) Zn/Al-CO_3^{2-}-LDH and (c, d) Zn/Al-SA-LDH

3.4 UV-Vis spectroscopy

The UV-vis absorbance and reflectance curves of SA, Zn/Al-SA-LDH and Zn/Al-CO_3^{2-}-LDH are displayed in Fig. 6(a). It can be seen that both SA and Zn/Al-SA-LDH have high absorbance values in the whole wavelength range. Specifically, the absorbance values are even more than 0.7 in the range of 240-300 nm. For Zn/Al-CO_3^{2-}-LDH, its absorbance curve fluctuates in the range of 0.1-0.15, which is much lower than SA and Zn/Al-SA-LDH absorbance values. On the other hand, the reflectance curves of Zn/Al-CO_3^{2-}-LDH and Zn/Al-SA-LDH are much higher than that of SA. To be specific, the reflectance values of Zn/Al-CO_3^{2-}-LDH and Zn/Al-SA-LDH are above 0.6 in the range of 230-320 nm. However, the reflectance curve of SA is maintaining at around 0.1. In view of the above results, it can be inferred that Zn-Al-SA-LDH has a synergistic effect of absorbing and reflecting UV light on bitumen. The mechanism of blocking UV light by Zn-Al-SA-LDH is illustrated in Fig. 6(b).

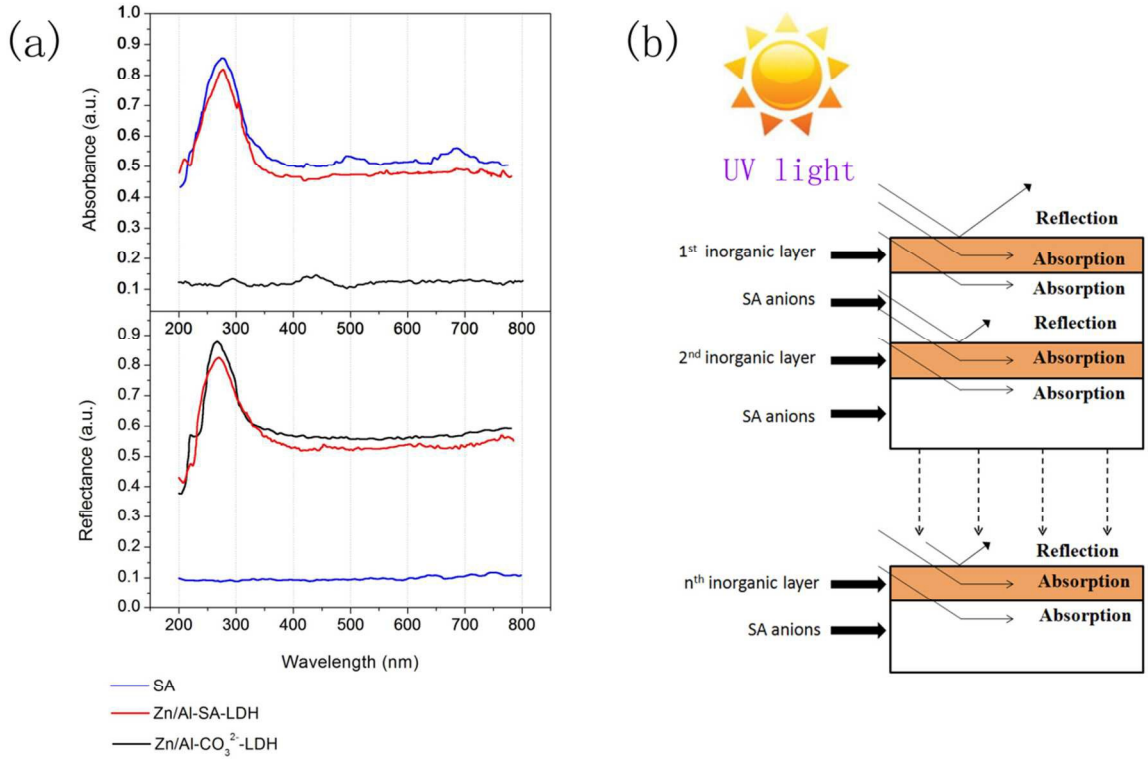

Fig. 6 (a) UV-Vis curves of SA, Zn/Al-CO_3^{2-}-LDH and Zn/Al-SA-LDH and (b) schematic illustration of absorbing and reflecting UV light by Zn/Al-SA-LDH

3.5 Physical Property

To evaluate the degradation of bitumen specimens, the penetration decrement ratio (PDR) and softening point increment ratio (SPIR) before and after UV aging are usually considered as important aging indexes.[19] PDR and SPIR can be calculated as the following equations:

$$PDR = \frac{Penetration\ before\ UV\ aging - Penetration\ after\ UV\ aging}{Penetration\ before\ UV\ aging} \times 100\% \quad (1)$$

$$SPIR = \frac{Softening\ point\ after\ UV\ aging - Softening\ point\ before\ UV\ aging}{Softening\ point\ before\ UV\ aging} \times 100\% \quad (2)$$

PDR and SPIR values of bitumen specimens are shown in Fig. 7. It can be seen that the PDR and SPIR values of Zn/Al-SA-LDH modified bitumen specimens are much lower than those values of other bitumen specimens. It indicates that Zn/Al-SA-LDH can significantly improve the UV aging resistance of modified bitumen.

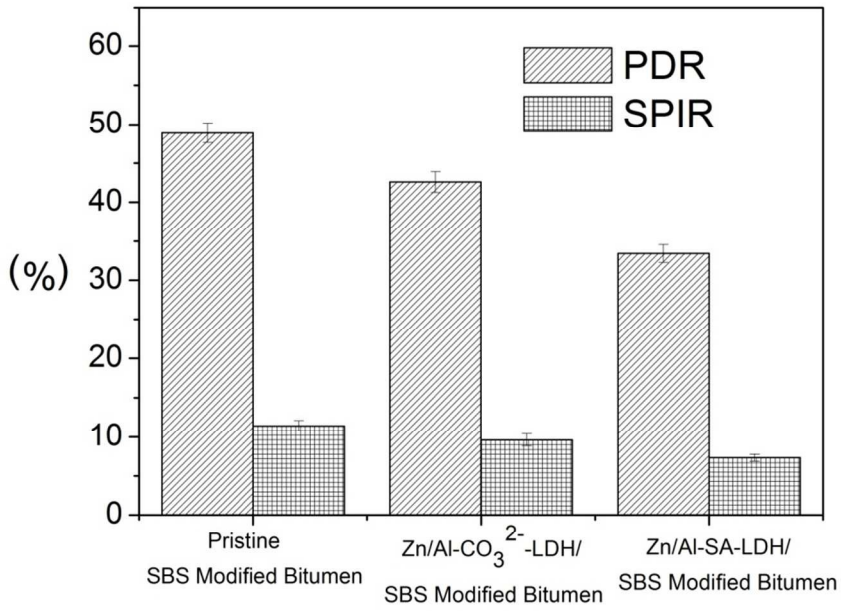

Fig. 7 UV aging indexes of bitumen specimens

3.6 FTIR analysis of bitumen before and after UV aging process

The complex chemical reactions occur during the UV aging process and the amount of some functional groups are subsequently changed. FTIR spectra can be used to calculate the functional group indexes of bitumen specimens before and after UV aging.[20] From

Fig. 8(a), it can be seen that the new broad and weak peaks appear at 3450 cm^{-1} in the spectra of Zn/Al-CO_3^{2-}-LDH/SBS modified bitumen and Zn/Al-SA-LDH/SBS modified bitumen. These peaks can be ascribed to the -OH groups and water molecules in the LDH galleries.[21] For both bitumen specimens, the strong peaks observed between 2923 cm^{-1} and 2852 cm^{-1} are caused by the antisymmetric and symmetric stretching vibrations of methyl groups in aliphatic chains. The peaks centered at 1600 cm^{-1} can be attributed to the vibrations of C=C bonds in aromatic fraction and the peaks at 1376 cm^{-1} can be ascribed to the symmetric deformation of -CH_3 groups or the antisymmetric deformation of -CH_2/-CH_3 groups. According to the previous researches,[22,23] the peaks at 1700 and 1030 cm^{-1} are attributed to the stretching vibrations of C=O bonds and S=O bonds. The oxidation due to the UV aging increases the amount of functional groups containing C=O and S=O, and thus the aging degree of bitumen specimens can be evaluated by C=O and S=O indexes. These two indexes are defined as the following equations.

$$C=O\ index=\frac{area\ of\ C=O\ band\ centered\ at\ 1700\ cm^{-1}}{total\ area\ of\ bands\ from\ 600\ cm^{-1}\ to\ 2000 cm^{-1}} \quad (3)$$

$$S=O\ index=\frac{area\ of\ S=O\ band\ centered\ at\ 1030\ cm^{-1}}{total\ area\ of\ bands\ from\ 600\ cm^{-1}\ to\ 2000\ cm^{-1}} \quad (4)$$

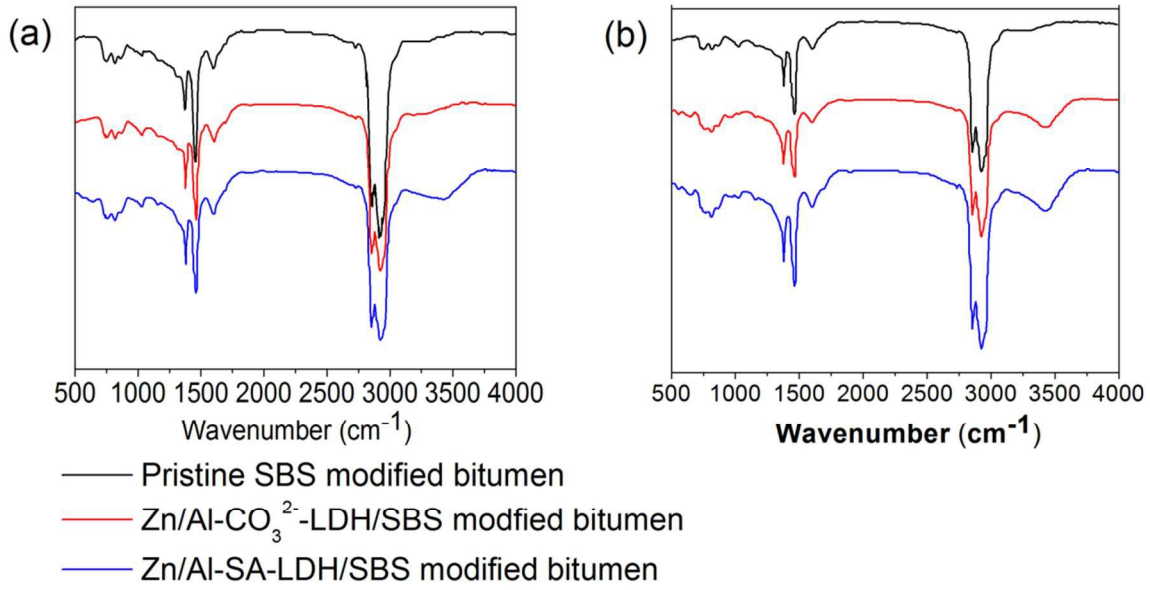

Fig. 8 FTIR spectra of bitumen specimens (a) before and (b) after UV aging process

The C=O and S=O indexes of bitumen specimens are listed in Table 1. After UV aging process, the increments of C=O and S=O indexes follow the order of pristine SBS modified bitumen > Zn/Al-CO_3^{2-}-LDH/SBS modified bitumen > Zn/Al-SA-LDH/SBS modified bitumen. That means less oxidation takes place in the aged Zn/Al-SA-LDH/SBS modified bitumen, and thus it provides an evidence that Zn/Al-SA-LDH can improve the UV aging resistance of bitumen more significantly.

Table. 1 Structure indexes of bitumen specimens before and after UV aging

Sample	C=O indexes			S=O indexes		
	Unaged	UV aged	Increment	Unaged	UV aged	Increment
Pristine SBS modified bitumen	0.00516	0.05323	0.04807	0.04512	0.08943	0.04431
Zn/Al-CO_3^{2-}-LDH/SBS modified bitumen	0.00509	0.04163	0.03654	0.04483	0.07369	0.02886
Zn/Al-SA-LDH/SBS modified bitumen	0.00521	0.03749	0.03228	0.04457	0.06524	0.02067

3.7 AFM observation

Topographic images of pristine SBS modified bitumen, Zn/Al-CO_3^{2-}-LDH/SBS modified bitumen and Zn/Al-SA-LDH/SBS modified bitumen are shown in Figs. 9(a, b, c). From Fig. 9(a), some "bee-like" wrinkles appear on the surface of pristine SBS modified bitumen. According to the previous researches, these wrinkles are caused by co-precipitates of microcrystalline waxes (carbon number > 40) and asphalten when hot melted bitumen cooled to room temperature.[24] As is shown in Fig. 9(b), the wrinkles in Zn/Al-CO_3^{2-}-LDH/SBS modified bitumen are obviously higher than those in pristine SBS modified bitumen. This is because the inorganic layers of Zn/Al-CO_3^{2-}-LDH lead to the stronger contractions between the wrinkles and organic bitumen matrix.[25] Fig. 9(c) shows that the wrinkles in Zn/Al-SA-LDH/SBS modified bitumen are lower than those in Zn/Al-CO_3^{2-}-LDH/SBS modified bitumen, indicating that Zn/Al-SA-LDH has a better compatibility with bitumen matrix due to the organic SA anions in LDH galleries.

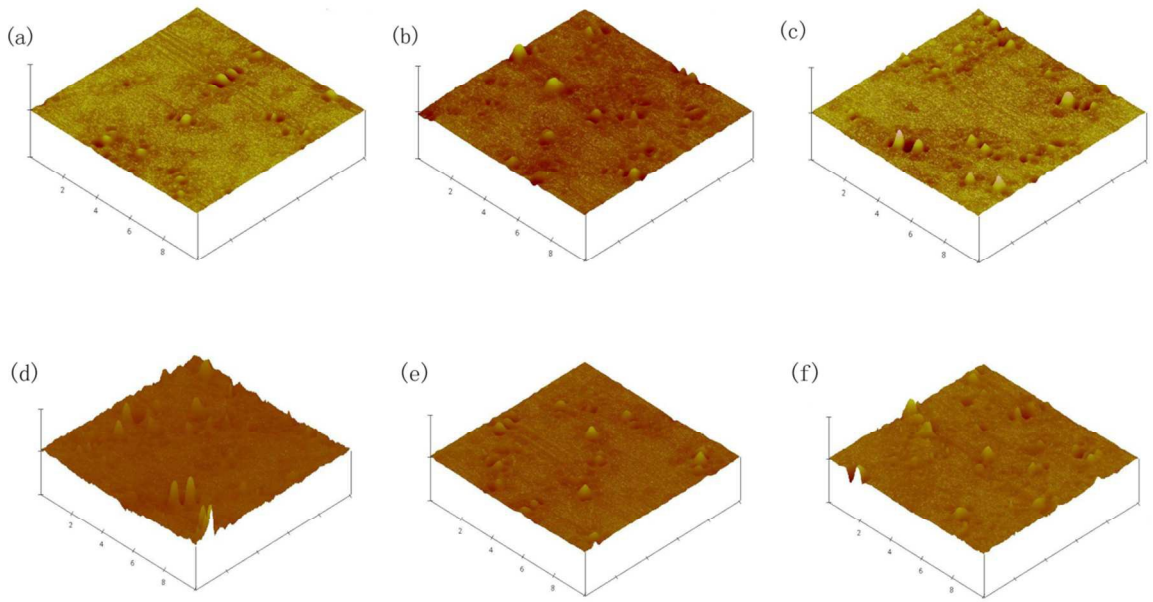

Fig. 9 Topographic images of (a, d) pristine SBS modified bitumen before and after UV aging, (b, e) Zn/Al-CO_3^{2-}-LDH/SBS modified bitumen before and after UV aging and (c, f) Zn/Al-SA-LDH/SBS modified bitumen before and after UV aging

After the UV aging process, topographic images of pristine SBS modified bitumen, Zn/Al-CO_3^{2-}-LDH/SBS modified bitumen and Zn/Al-SA-LDH/SBS modified bitumen are shown in Figs. 9(d, e, f). From Fig. 9(d), the heights of the wrinkles in pristine SBS modified bitumen rise remarkably after aging. This is because some short fragments are generated due to the breakdown of polystyrene and polybutadiene segments under the UV radiation.[26] These segments occupy larger space than the organic molecules in bitumen, resulting in a rough surface of bitumen. The heights of wrinkles in Fig. 9(e) increase slightly after aging, indicating that Zn/Al-CO_3^{2-}-LDH can somewhat block the UV radiation. The heights of wrinkles in Fig. 9(f) do not change during the aging process, implying that Zn/Al-SA-LDH can effectively improve UV aging resistance of SBS modified bitumen.

Phase images of pristine SBS modified bitumen, Zn/Al-CO_3^{2-}-LDH/SBS modified bitumen and Zn/Al-SA-LDH/SBS modified bitumen are shown in Figs.10(a, b, c). From Fig.10 (a), two phases including homogeneous matrix and dispersed units can be seen in pristine SBS modified bitumen. Fig. 10(b) depicts that the contrast between these two phases increases remarkably due to the formation of separated structure in Zn/Al-CO_3^{2-}-LDH/SBS modified bitumen. Compared with Zn/Al-CO_3^{2-}-LDH, Zn/Al-SA-LDH decreases the phase contrast to some extent (shown in Fig. 10(c)). This is because the bitumen molecules containing benzene rings have the similar polarity with SA anions in LDH galleries.

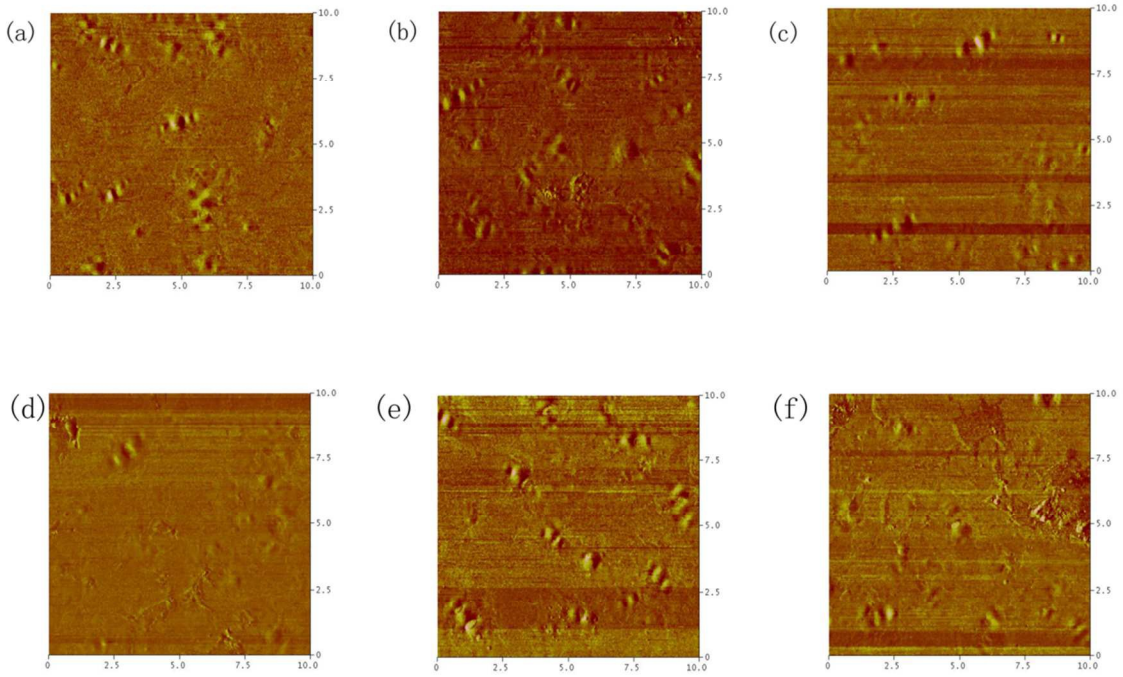

Fig.10 Phase images of (a, d) pristine SBS modified bitumen before and after UV aging, (b, e) Zn/Al-CO_3^{2-}-LDH /SBS modified bitumen before and after UV aging and (c, f) Zn/Al-SA-LDH/SBS modified bitumen before and after UV aging

The phase images of pristine SBS modified bitumen, Zn/Al-CO_3^{2-}-LDH/SBS modified bitumen and Zn/Al-SA-LDH/SBS modified bitumen after UV aging process are exhibited in Figs. 10(d, f, g). From Fig. 10(d), it can be seen that the number of "bee-like" wrinkles decreases significantly in aged pristine SBS modified bitumen. Besides, the boundary line between two phases becomes blurred. It can be associated with the increased polarity by the formation of hydroperoxide, alcohol and hydroxyl, acidic, carboxyl and ketonic function groups in bitumen matrix during the aging process.[27,28] The overall polarity of bitumen matrix increased remarkably due to the above functional groups, and thus the contrast tends to be decreased between bitumen matrix and dispersed units. Figs. 10(e) and (f) display that the phase difference in Zn/Al-SA-LDH modified bitumen is more obvious than that in Zn/Al-CO_3^{2-}-LDH modified bitumen. That means the addition of Zn/Al-SA-LDH can retard the trend of single phase in bitumen, and thereby the UV aging resistance can be evidently improved.

4. Conclusions

SA anions was introduced into LDH galleries by calcination recovery method, and then the effects of Zn/Al-CO_3^{2-}-LDH and Zn/Al-SA-LDH on UV aging resistance of SBS modified bitumen were investigated. Some conclusions can be drawn as follows:

(1) FTIR and XRD results indicate that SA anions have be intercalated into the layers of Zn/Al-LDH and the interlayer distance of LDH layers increased from 0.76 nm to 1.54 nm. Meanwhile separated and expanded structures are formed in Zn/Al-CO_3^{2-}-LDH/SBS modified bitumen and Zn/Al-SA-LDH/SBS modified bitumen, respectively. UV-vis curves display that the Zn/Al-SA-LDH plays a synergistic role of reflecting and absorbing the UV light.

(2) Physical property tests show that PDR and SPIR of Zn/Al-SA-LDH/SBS modified bitumen are lower than those of Zn/Al-CO_3^{2-}-LDH/SBS modified bitumen. FTIR analysis of function groups manifests that the generation of S=O and C=O groups in Zn/Al-SA-LDH/SBS modified bitumen can be effectively prohibited during UV aging process. AFM images directly display that Zn/Al-SA-LDH can retard the trend of single phase in bitumen matrix, indicating that the introduction of Zn/Al-SA-LDH can enhance the UV aging resistance of SBS modified bitumen remarkably.

Acknowledgements

This research is supported by the National Basic Research Program of China (2014CB932104) and the National Key Technology Research and Development Program of the Ministry of Science and Technology of China (2011BAE28B04).

References

1 P. Redelius and H. Soenen, *Fuel*, 2015, **140**, 34-43.

2 N. Dehouche, M. Kaci and K. A. Mokhtar, *Constr. Build. Mater.*, 2012, **26**, 350-356.

3 F. Durrieu, F. Farcas and V. Mouillet, *Fuel*, 2007, **86**, 1446–1451.

4 X. Lu and U. Isacsson, *Fuel*, 1998, **77**, 961-972.

5 P. De Filippis, C. Giavarini and M. Scarsella, *Fuel*, 1995, **74**, 836-841.

6 C. Ouyang, S. Wang, Y. Zhang and Y. Zhang, *Polym. Degrad. Stabil.*, 2006, **91**, 795-804.

7 S. Dessouky, D. Contreras, J. Sanchez and A.T. Papagiannakis, *Constr. Build. Mater.*, 2013, **38**, 214-223.

8 P. Cong, P. Xu and S. Chen, *Constr. Build. Mater.*, 2014, **52**, 306-313.

9 J. Yu, L. Wang, X. Zeng, S. Wu and B. Li, *Polym. Eng. Sci.*, 2007, **47**, 1289-1295.

10 Y. F. Huang, Z. G. Feng, H. L. Zhang and J. Y. Yu, *J. Test. Eval.*, 2012, **40**, 734-739.

11 X. Zhang, L. Zhou, H. Pi, S. Guo and J. Fu, *Polym. Degrad. Stabil.*, 2014, **102**, 204–211.

12 Q. Wang, J. Wu, Y. Gao, Z. Zhang, J. Wang, X. Zhang, X. Yan, A. Umar, Z. Guo and D. O'Hare, *RSC. Adv.*, 2013, **3**, 26017-26024.

13 O. Saber, *Polym. Bull.*, 2012, **68**, 209-222.

14 Q. Wang, Y. Gao, J. Luo, Z. Zhong, A. Borgna, Z. Guo and D. O'Hare, *RSC. Adv.*, 2013, **3**, 3414-3420.

15 J. Yu, X. Zeng, S. Wu, L. Wang and G. Liu, *Mater. Sci. Eng. A.*, 2007, **447**, 233-238.

16 B. Wang, H. Zhang, D. G. Evans and X. Duan, *Mater. Chem. Phys.*, 2005, **92**, 190-196.

17 A. M. Alansi, W. Z. Alkayali, M. H. Al-qunaibit, T. F. Qahtan and T. A. Saleh, *RSC. Adv.*, 2015, **5**, 71441-71448.

18 N. Iyi, Y. Ebina and T. Sasaki, *J. Mater. Chem.*, 2011, **21**, 8085-8095.

19 H. Zhang, J. Yu, D. Kuang, *Constr. Build. Mater.*, 2012, **26**, 244-248.

20 Z. Feng, H. Bian, X. Li and J. Yu, *Mater. Struct.*, 2015, **3**, 1-9.

21 G. Wang, S. Xu, C. Xia, D. Yan, Y. Lin and M. Wei, *RSC. Adv.*, 2015, **5**, 23708-23714.

22 S. Wu, L. Pang, L. Mo, Y. Chen and G. Zhu, *Constr. Build. Mater.*, 2009, **23**, 1005-1010.

23 F. Zhang, J. Yu and J. Han, *Constr. Build. Mater.*, 2011, **25**, 129-137.

24 H. Zhang, H. Wang and J. Yu, *J. Microsc.*, 2011, **242**, 37-45.

25 H. Zhang, J. Yu, L. Xue and Z. Li, *J. Microsc.*, 2011, **244**, 85-92.

26 U. Isacsson and H. Zeng, *Mater. Struct.*, 1998, **31**, 58-63.

27 R. P. Singh, S. M. Desai, S. S. Solanky and P. N. Thanki, *J. Appl. Polym. Sci.*, 2000, **75**, 1103-1114.

28 X. Lu and U. Isacsson, *Constr. Build. Mater.*, 2002, **16**, 15-22.